PAKISTAN INSTITUTE OF CHEMICAL ENGINEERS
Since 1969

Journal of Pakistan Institute of Chemical Engineers

Journal homepage: www.piche.org.pk/journal

DOI: https://doi.org/10.54693/piche.05112

Check for updates

Fabrication of Solar Cells using $ZnO/MnO_2/CdS$ Nanocomposite as a Catalyst

S.A. Noor[1], A.J. Al-Shamari[2], M.M. Alrufaie[3]

Submitted: 14/04/2023, Accepted: 18/05/2023, Online: 22/05/2023

Abstract

The nanoparticles prepared in this study were used by hydrothermal chemical method to generate dye-sensitive cells (dye-sensitized solar cells) (DSSCs), which were ternary nanocomposite $ZnO/MnO_2/CdS$ and also used as photoelectrodes using two natural dyes as absorbent medium: red (Hibiscus sabdariffa), and green (Apium graveolens). The ternary nanocomposite ($ZnO/MnO_2/CdS$) was prepared, and the results also showed that the green dye efficiency in DSSCs with the prepared nanosurface is greater than the red dye in terms of conversion efficiency (ç), and the ternary nanocomposite was also diagnosed and characterized by examining the properties of nanomaterials Prepared by X-ray diffraction (XRD), scanning electron microscopy (FE-SEM), and transmission electron microscopy (TEM) was used to analyze $ZnO/MnO_2/CdS$ which shows the nature of the surface as well as the surface area it provides. The purpose of the study is to improve the performance of dye solar cells and develop their work in the future. The sizes of the $ZnO/MnO_2/CdS$ nanocomposite particles were also studied. Where the sizes of the prepared nanomaterials were within the nano size range.

Keywords: Solar cells, **N**anocomposite, DSSCs**,** Photoelectrodes**,** Photovoltaic, Conversion efficiency ( ).

1. Introduction:

Many energy storage solutions are needed in the contemporary environment due to the growing depletion of nonrenewable energy resources. versus the typical electrolytic capacitor [1,2]. A new type of energy storage device has recently become very popular in several industrial scaleup sectors, such as solar energy panels, mobile devices, and sudden spikes in power demand [3,4]. Its lower energy density compared to solar cells and batteries restricts its full exploitation for useful purposes. widening voltage and boosting electrode material capacity, can effectively improve low energy. On the other hand, power density can be increased thanks to the electrode's high conductivity and low charge-transfer resistance [5,6]. The performance is greatly influenced by the mechanical characteristics and stability of an electrode material [7-9]. Intriguing electrode materials for electrochemistry include transition metal oxides. Transition metal oxides with higher specific capacitance and energy density include (MnO_2, ZnO, and CdS) [10,11]. MnO_2, a nontoxic transition metal oxide that was recently acquired and has a high theoretical capacitance,

[1]*College of Pharmacy, University of Kufa,Al- Najaf / Iraq.*
[2,3]*College of Science, ,[2] ,University of Kufa, ,Al- Najaf / Iraq.*
Corresponding Author: muhaimin.alrufaie@uokufa.edu.iq

has drawn a lot of attention because of its affordability, strong electrochemical reactivity, environmentally benign characteristic, and improved operational safety. Although one of the most tempting options, MnO2 has faced considerable challenges because of its poor rate performance and low electrical conductivity, which limit its rate potential for high power and cycle performances. Morphology, specific surface area, and electrical conductivity have a big impact on how much capacitance may be obtained [12]. As prospective methods to increase the electrochemical performance of MnO_2 to enhance electrical conductivity, a variety of MnO_2-conductive matrices (carbonaceous materials and conducting polymers) hybrid nanostructures have been proposed. By enhancing electrical conductivity, these methods could enhance the electrochemical performance of the electrode material. Among various semiconductor photocatalysts, ZnO is one of the intensively studied photocatalysts due to its low cost, nontoxic nature, high quantum efficiency, and environmental friendly [1315]. Several systems, such as doping, surface modification using metal nanoparticles, and heterostructure development, have been used to address ZnO shortcomings [1618]. For photocatalytic applications, a mixture of ZnO/CdS nanocomposites [19] has been used to improve light absorption and offer efficient charge transport. Due to dimensional anisotropy, which is one of these morphologies' many benefits, the maximum number of charge High optical absorption coefficient transition metal sulfide CdS [20]. According to numerous reports, the formation of binary composites, such as ZnO-CdS, is to blame for the increase in photocatalytic activity in the visible range [21]. Nanocomposites have a number of advantages, including high charge separation, the ability to serve as a substrate for heterogeneous nucleation, high charge carrier mobility, and an extended charge carrier lifetime [22].

Brian O'Regan and Michael Gratzel developed the DSSC idea in 1991 using mesoporous TiO2 nanoparticles and ruthenium dye [23], and the system's best photoconversion efficiency is 14.3% [24]. This review discusses various photovoltaic technologies, their operating theories, the fabrication of photovoltaic devices using a variety of novel inorganic nanostructured materials, and the factors that affect the performance of DSSC devices, including photoconversion efficiency (PCE), short circuit current (J_{sc}), open-circuit voltage (V_{oc}), and fills factor (FF).

2. Experimental Part:

This work deals with the process of preparation of photocatalyst $ZnO/MnO_2/CdS$, characterization techniques, and the experimental set-up used for the Fabrication of Solar Cells using triple nanocomposite as a catalyst.

2.1. Used Chemicals:

[Zn $(NO_3)_2.6H_2O$, Cd $(NO_3)_2.4H_2O$, SC $(NH_2)_2$, HMT (Hexamethylenetetramine or methenamine), MnO_2, and PVP].

2.2. A New Method For Preparing $ZnO/MnOo_2/CdS$ Nanocomposites By Hydrothermal Method:

Tri-Nanocomposite (ZnO/MnO2/CdS) is prepared in many processes. The first step involves mixing the materials [Zn $(NO_3)_2.6H_2O$, Cd $(NO_3)_2.4H_2O$, SC $(NH_2)_2$, HMT, MnO_2, and PVP] in a 1:1 ratio for each. Step 2: Stir continuously for 30 min. while combining the aforementioned ingredients with the least amount of deionized water (DIW). This answer is graded as an A.

Step 3: Create a B solution of sodium hydroxide, or NaOH, in a volume of 30 ml at a concentration of 5 M. Add a drop while stirring continuously for a further 30 minutes at pH = 12. Place in the autoclave and heat to 200 °C for 12 hours. After centrifuging to separate, repeat numerous washes in deionized water, and dry in a 70 °C. oven. After that, two hours of calcination at 450 °C.

2.3. Characterization Of Prepared Compounds:

2.3.1. XRD Analysis:

X-ray diffraction diffractogram of ZnO/ MnO_2/CdS nanocomposites is depicted, which shows highly intense but narrow peaks. The XRD patterns observed at 31.74 (100), 34.11 (002), 36.22 (101), 47.51(102), 56.54 (110), 62.83 (103), 67.90 (112), 69.02 (201), 76.89 (202),81.36 (104), 89.55 (203) correspond to the crystalline lattice planes (h k l) and by comparing to the standard diffraction data from JCPDS-01-078-4498 [25]. ZnO/MnO_2/CdS nanocomposites have a cubical and hexagonal crystal shape and the Debye Scherrer's estimated average crystallite size (D) was 32.9 nm. The calculated average crystallite size gives supporting evidence for the ZnO/MnO_2/CdS nanocomposites in the nanoscale.

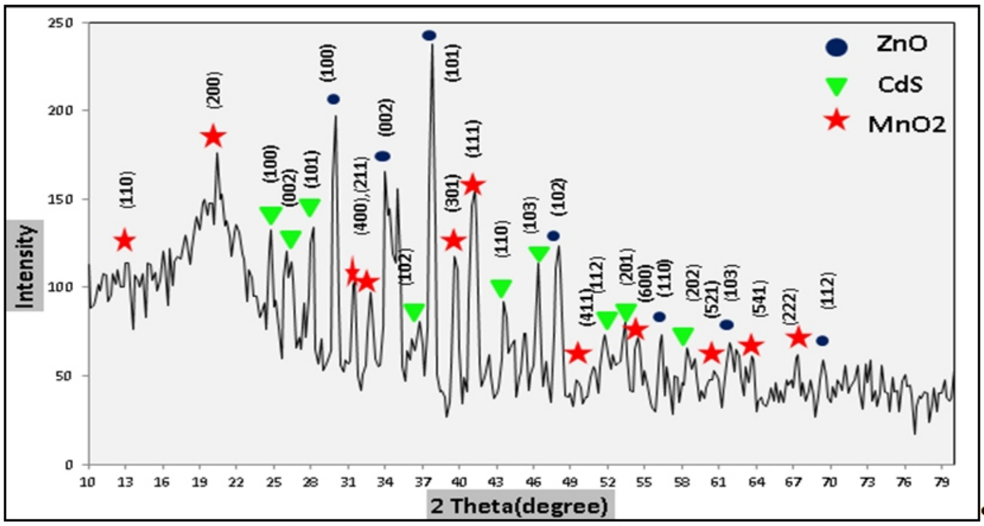

Figure (2-1): X-Ray Diffraction pattern of ZnO/MnO_2/CdS nanocomposite

2.3.2. FE-SEM Analysis:

The surface structures of the developed ZnO / MnO_2 / CdS nanocomposite were analyzed using SEM and the microscopic images are shown in Figure (2-2). The morphology of ZnO / MnO_2 / CdS was observed, forming a regular mixture of spherical and rod shapes for (ZnO) and (MnO_2) and (CdS) in the form of clearly visible clusters as in the figure, and the average diameter of the nanoparticles was determined to be (18.13 nm), with an approximate size range from (10 to 30 nm). The images show the size, shape, and way the nanoparticles clump together.

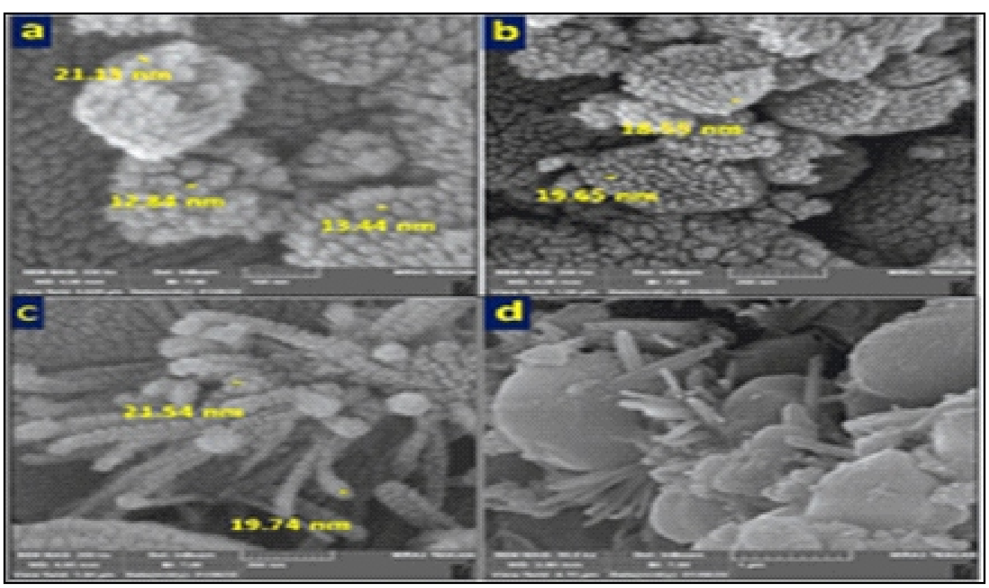

Figure (2-2): Shows images FE-SEM of ZnO/MnO_2/CdS triple Nanocomposite

2.3.3. Transmission Electron Microscopy (tem) Analysis:

Transmission electron microscopy (TEM) of the $ZnO/MnO_2/CdS$ nanocomposite produced by the hydrothermal process typically shows irregular shapes with nanopores on its surface as observed in Figure (2-3). The micro outer layer images indicate the catalytic sites of the $ZnO/MnO_2/CdS$ nanocomposite. The figure also shows at different magnifications the presence of catalytic active sites with different orientations for $ZnO / MnO_2 /CdS$ nanocomposite crystals were indicated on the surface, which may enhance the redox reaction rate for active detection of a biomolecule. Figure (2-3) also shows the size of and the formation of the triple nanocomposite $ZnO / MnO_2 / CdS$, the particles of which range in size within (10.77 - 88 nm).

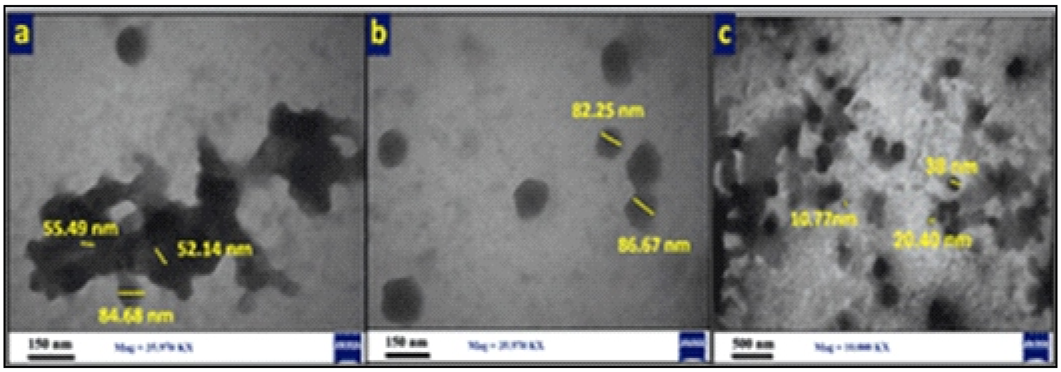

Figure (2-3): shows images TEM of $ZnO/MnO_2/CdS$ nanocomposite

2.3.4. Atomic Forcr Microscope (afm) Analysis:

The shape of the nanoparticles of the $ZnO/MnO_2/CdS$ nanocomposite is estimated on the basis of AFM images and line scans, and Figure (2-4) shows the AFM image of the $ZnO/MnO_2/CdS$ nanocomposite whose RMS roughness value for the as-prepared samples was 6.705 nm for a scanned area of 1 × 1 ìm and this value was verified using section line analysis. The results show 2D and 3D rendering for the sample surface at micrometer and nanometer scale, the image result shows a 2D AFM filter for nanocomposite particles using a font profile. The size distribution of particles and nanocomposites is displayed in the picture and table (2-1) below, the produced nanocomposite's parameters are also shown in the table.

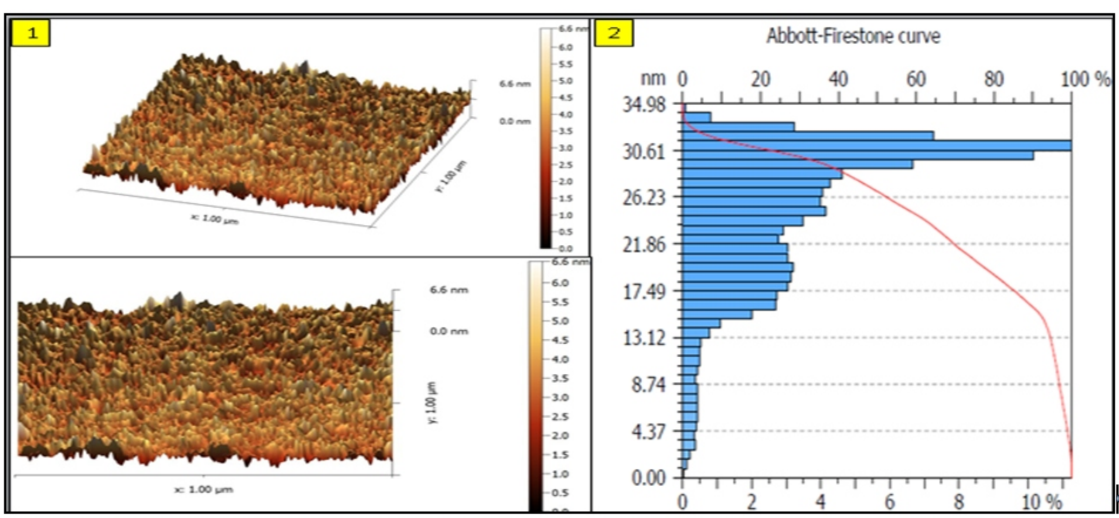

Figure (2-4): AFM (1) 2D and 3D image and (2) particles size distribution of prepared $ZnO/MnO_2/CdS$ nanocomposite by hydrothermal method

Table 2.1: AFM parameters of synthesized nanoparticles and nanocomposite

Compound	Roughness Average Sa (nm)	Root Mean Square height S_q (nm)	Maximum height S_z (nm)	Developed interfacial area ratio S_{dr}(%)
$ZnO/MnO_2/CdS$	5.501	6.705	34.98	6.332

3. Fabrication of Dye-sensitized Solar Cells Using the $ZnO/MnO_2/CdS$ Tri-Nanocomposite as a Catalyst:

Third-generation or emerging photovoltaic. Researchers began developing a third generation of solar cells, also known as emerging photovoltaics, in order to avoid the drawbacks of first and second-generation solar cells. The following categories apply to emerging photovoltaics: -

- Dye-sensitized solar cells (DSSC)
- Quantum dot solar cells - Bulk heterojunction solar cells (QDSSC)

Solar cells are made of perovskites.

Dye-Sensitized Solar Cells. The architecture of DSSC contains a mesoporous wide bandgap semiconductor material (typically $ZnO/MnO_2/CdS$) that sensitizes a monolayer of dyes (Two natural dyes) and a liquid electrolyte with an anti-carbon electrode counter electrode. In DSSC, $ZnO/MnO_2/CdS$ acts as a scaffolding layer for dye molecules and also facilitates charge collection and conduction. The main features of $ZnO/MnO_2/CdS$ are it is low-cost, abundant, stable, and photoactive.

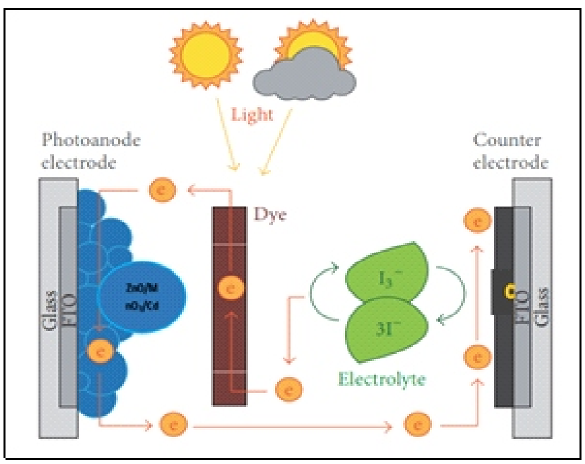

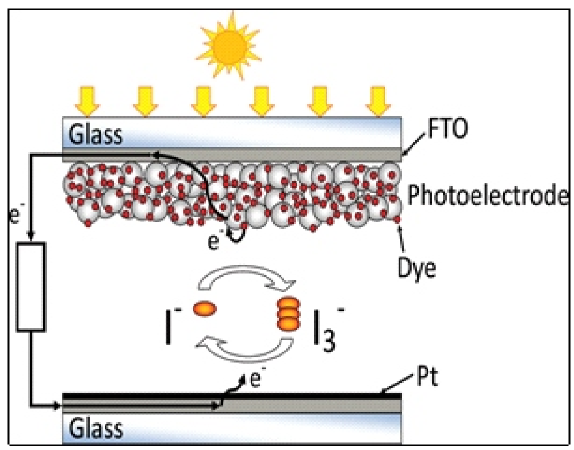

Several TCOs are being developed, but the two that perform the best are fluoride-doped tin oxide and indium oxide with tin doping (ITO) (FTO). FTO substrates are superior to ITO for DSSC because they are less expensive and more stable up to 550C°, although FTO has lower optical transparency and electrical conductivity. ZnO is the best alternative for DSSC photonic fabrication. The band gap in ZnO is (3.29 eV). The mobility and carrier lifetime of electrons in ZnO is higher which is an important feature of DSSC [26]. The synthesis of ZnO is very easy and the growth of different morphologies. Current status of photoconversion efficiency of DSSC. But ZnO dissolves in the iodide/triiodide electrolyte and forms Zn^{2+} ions and thus reduces the efficiency. To overcome the limitations of ZnO in the presence of the redox iodide/tertiary electrolyte, multilayer double hydroxide was studied as photoresist for DSSC [27,28]. There are still options for new structures/materials/architecture for the excellent performance of DSSC by overlaying ZnO with MnO_2, CdS to improve the conversion efficiency of the solar cell. The primary function of a solar cell is to convert sunlight into electricity, which is accomplished by the J-V properties of DSSC. We can determine the P_{max}, which stands for the maximum deliverable power, using the J-V curve. The following expression is used to compute the DSSC's fill factor.

$$FF = \frac{P_{Max}}{V_{oc} \times I_{SC}} \quad (1)$$

$$= \frac{V_{oc} \times J_{SC} \times FF}{E} \quad (2)$$

$$FF = \frac{V_{Max} \times J_{Max}}{V_{oc} \times J_{SC}} \quad (3)$$

Shunt and series resistance are shown to be limiting factors in solar cells [29]. High fill factor FF is caused by large shunt resistance and low series resistance in solar cells. Energy conversion effectiveness (ç)The difference between the delivered power (P_{max}) and incident light power is what is known as a DSSC's efficiency (P_{in}). The following expression is used to compute the solar cell's photoconversion efficiency;

$$\% = \frac{V_{oc} \times J_{SC} \times FF}{P_{in}} \quad (4)$$

DSSCs were created using a nanocomposite ($ZnO/MnO_2/CdS$) that was created for the study and employed as a photoelectrode with two natural dyes as absorbent media: red dye (from the Roselle plant or Hibiscus sabdarriffa) and green dye (from Apium graveolens). The I-V and characteristics of DSSCs made from nanosurfaces and natural dyes are shown in Figures (3-1) and (3-2). Whereas, as shown in Table (3-1) the results indicated that the DSSC with the green dye is more effective in terms of conversion efficiency (ç) than the red dye. There are various causes, one of which is the energy gap, which is different for the red and green dyes and is larger for the green dye. As a result, more ray wavelengths penetrate the cells and are absorbed by the dye [30]. Second, the triple nanocomposite surface area, as everyone of us has a unique surface area. The effectiveness of the constructed DSSC rises as the green dye's adsorption on nanoscale surfaces increases. Moreover, due to the increased concentration of natural dye impurities, the current yield of DSSC made with the red natural dye is lower than that of DSSC made with the green dye [31]. Also, the low intensity (22.53 mW/cm^2) of the light source used is another factor contributing to the low value found for the manufactured DSSCs.

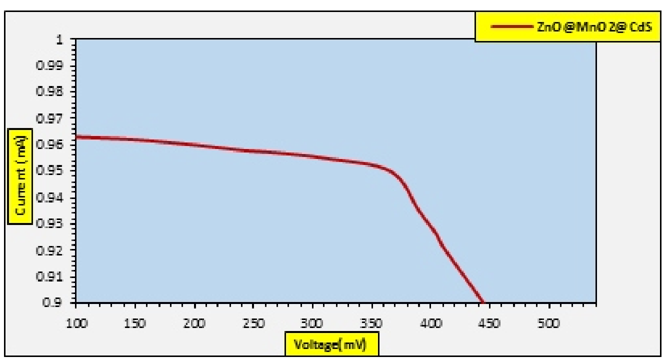

Figure (3.1): I-V characteristics of prepared DSSCs nanoparticles and Nanocomposite prepared with red dye (Roselle).

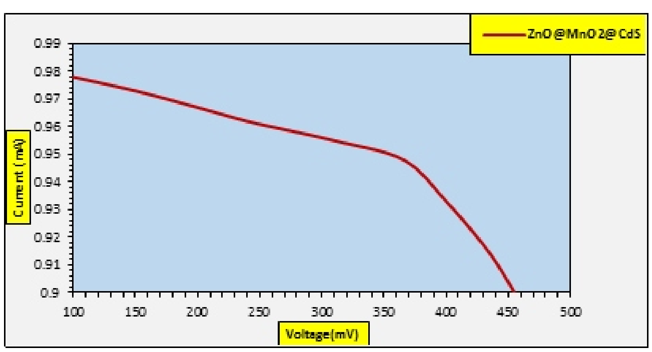

Figure (3.2): I-V characteristics of prepared DSSCs nanoparticles and Nanocomposite prepared with green dye (Apium graveolens)

Table 3.1: Photo electrochemical parameters of DSSCs, (A=5.4cm^2 red dye, 4.5 cm^2 green dye) under light intensity) 22.53 mW/cm^2

Catalyst/Dye		I_{SC} (mA)	V_{oc} (V)	I_{max} (mA)	V_{max} (V)	P_{max}	FF	η %
ZnO@MnO_2/CdS	Rad dye	0.963	445	0.952	365	347.48	0.8109	0.6435
	Green dye	0.978	455	0.948	370	350.76	0.788	0.7795

Figure 3.3: Pictures while examining the solar cells with the Keithly apparatus

4. Conclusion And Future Perspectives:

Abstract: Preparation of ZnO/MnO2/CdS ternary nanocomposite particles using simple chemical methods such as the one-step hydrothermal process. ZnO/MnO2/CdS nanocomposite particles have been used as electrodynamic catalysts, and the effectiveness of nanomaterials (semiconductors) in the formation of dye-sensitized cells (DSSCs) has also been verified, as well as the use of solar cells in daily life applications due to their wide properties in terms of surface area and small size. And the effectiveness it provides, which depends on the nature of the prepared surface.

Using two natural dyes of different color with dye-sensitive cells (DSSCs) and studying the comparison between the two dyes in terms of conversion efficiency (ç) for solar cells and which one is more efficient in conversion, as the results showed the effectiveness of the green dye when compared to the red dye with solar cells, where dyes were used [Red (Hibiscus sabdariffa) and green (Apium Gravolens)]. One of the benefits of using different characterizations is to know the nature of nanomaterials surfaces, their sizes and their effectiveness as photoelectrodes.

References:

1. M.Z.U. Shah et al, A Novel TiO2/CuSe Based Nanocomposite for High-Voltage (2.2 V), Asymmetric Supercapacitors. (2022) 100418.

2. C. Liu, Y. Bai, W. Li, F. Yang, G. Zhang, H. Pang, In Situ Growth of ThreeDimensional MXene/MetalOrganic Framework Composites for High-Performance Supercapacitors, Angewandte Chemie 134 (11) (2022) e202116282.

3 .Chen, S., et al., Graphene oxide- MnO2

nanocomposites for supercapacitors. 2010. 4 (5): p. 2822-2830.

4. Y. Bai, C. Liu, T. Chen, W. Li, S. Zheng, Y. Pi, Y. Luo, H. Pang, MXene-copper/cobalt hybrids via lewis acidic molten salts etching for high performance symmetric supercapacitors, Angewandte Chemie 133 (48) (2021) 2552225526.
5. J.K. Chang et al., Pseudocapacitive mechanism of manganese oxide in 1-ethyl-3-methylimidazolium thiocyanate ionic liquid electrolyte studied using X-ray photoelectron spectroscopy. 2009. 25(19): p. 11955-11960.
6. C. He, J. Cheng, Y. Liu, X. Zhang, B. Wang, Thin-walled hollow fibers for flexible high energy density fiber-shaped supercapacitors, Energy Materials (2021) 100010.
7. X. Zhou and L.J.T.S.F. Ma, MnO_2/ZnO porous film: Electrochemical synthesis and enhanced supercapacitor performances. 2015. 597: p. 44-49.
8. H. Gao, H. Shen, H. Wu, H. Jing, Y. Sun, B. Liu, Z. Chen, J. Song, L. Lu, Z. Wu, Q. Hao, Review of pristine Metal-Organic Frameworks for supercapacitors: recent progress and perspectives, Energy & Fuels 35 (16) (2021) 1288412901.
9. C. Li et al., Fabricating an aqueous symmetric supercapacitor with a stable high working voltage of 2 V by using an alkalineacidic electrolyte. Advanced Science, 2019. 6(1): p. 1801665.
10. T. Brezesinski et al., Ordered mesoporous á-MoO3 with iso-oriented nanocrystalline walls for thin-film pseudocapacitors. 2010. 9(2): p. 146-151.
11. L. Zhu, Z. Chang, Y. Wang, B. Chen, Y. Zhu, W. Tang, Y. Wu, Coreshell MnO 2@ Fe 2 O 3 nanospindles as a positive electrode for aqueous supercapacitors, Journal of Materials Chemistry A 3 (44) (2015) 2206622072.
12. L. Yuan, X.-H. Lu, X.u. Xiao, T. Zhai, J. Dai, F. Zhang, B. Hu, X. Wang, L.i. Gong, J. Chen, C. Hu, Y. Tong, J. Zhou, Z.L. Wang, Flexible Solid-State Supercapacitors Based on Carbon Nanoparticles/MnO 2 Nanorods Hybrid Structure, Flexible solidstate supercapacitors based on carbon nanoparticles/MnO2 nanorods hybrid structure. 6 (1) (2012) 656661.
13. B. Su, M. Zhong, L. Han et al., Eco-friendly preparation of hierarchically selfassembly porous ZnO nanosheets for enhanced photocatalytic performance. Mater. Res. Bull. 124, 110777110781 (2020).
14. A. Serr` a, P. Pip, E. Gomez, ´ et al., Efficient magnetic hybrid ZnO-based photocatalysts for visiblelight-driven removal of toxic cyanobacteria blooms and cyanotoxins. Appl. Catal. B 268, 118745 (2020)
15. J. Qiu, M. Li, Y. Wan et al., One-pot fabrication of CdxZn1-xS/ZnO nanohybrid using mixed sulfur sources for photocatalysis. Mater. Res. Bull. 125, 110776110782 (2020).
16. Y.-Q. Li, S.-Y. Fu, Y.-W. Mai, Preparation and characterization of transparent ZnO/epoxy nanocomposites with high-UV shielding efficiency. Polymer 47(6), 21272132 (2006).
17. V.H.T. Thi, B.-K. Lee, Great improvement on tetracycline removal using ZnO rod-activated carbon fiber composite prepared with a facile microwave method. J. Hard Mater. 324, 329339 (2017).
18. A. Akhundi, A. Habibi-Yangjeh, Ternary magnetic g-C3N4/Fe3O4/AgI nanocomposites: novel recyclable photocatalysts with enhanced activity in degradation of different pollutants under visible light. Mater. Chem. Phys. 174, 5969 (2016).
19. M. Zirak, O. Moradlou, M. Bayati et al., On the growth and photocatalytic activity of the vertically aligned ZnO nanorods grafted by CdS shells. Appl. Surf. Sci. 273, 391398 (2013).
20. P. Gao, J. Liu, T. Zhang et al., Hierarchical TiO2/CdS “spindle-like” composite with high photodegradation and antibacterial capability under visible light irradiation. J. of Hazar Mater. 229 230, 209216 (2012).
21. M. Zirak, O. Akhavan, O. Moradlou, Vertically aligned ZnO@ CdS nanorod heterostructures for visible light photoinactivation of bacteria.

J. of Alloys and Compounds 590, 507513 (2014) Page 14/16.

22. T. Jana, A. Pal, K. Chatterjee, Self assembled flower like CdSZnO nanocomposite and its photo catalytic activity. J. of Alloys and Compounds 583, 510515 (2014).
23. B. O'Regan, M. Gratzel, Nature 353 (1991) 737.
24. K. Kakiage, Y. Aoyama, T. Yano, K. Oya, J.-I. Fujisawa, M. Hanaya, Chem. Commun. 51 (2015) 1589415897.
25. S. Sharma, P. Chauhan and S. Husain, Materials Research Express PAPER Liquefied petroleum gas sensor based on manganese (III) oxide and zinc manganese (III) oxide nanoparticles, Materials Research Express PAPER Liquefied petroleum gas sensor based on manganese (III) oxide and zinc manganese (III) oxide nanoparticles, Published 4 January 2018 , Volume 5, Number 1.
26. Mustafa Biçer, Muharrem Gökçen, Ersin Orhan, Fabrication and photoanode performance of ZnO nanoflowers in ZnO-based dye-sensitized solar cells, Available online 9 July 2022, Version of Record 9 July 2022.
27. S. Liu, J. Liu, T. Wang, C. Wang, Z. Ge, J. Liu, X. Hao, N. Du, H. Xiao, Colloids Surf., A 568 (2019) 59-65.
28. L.J. Foruzin, Z. Rezvani, K. Nejati, Sol. Energy 186 (2019) 106112.
29. A. Onno, C. Chen, P. Koswatta, M. Boccard, Z.C. Holman, J. Appl. Phys. 126 (2019) 183103.
30. P. Thickness, S. Plasmon, H. Jaafar, R. M. Rosnan, H. Yahaya, and S. S. Abdullah, “Enhancing Photocurrent Performance Based on DyeSensitized Solar Cells,” vol. 12, no. 2111, pp. 114, 2019.
31. L. Schöttner, A. Nefedov, C. Yang, S. Heissler, and Y. Wang, “Structural Evolution of á -Fe 2 O 3 (0001) Surfaces Under Reduction Conditions Monitored by Infrared Spectroscopy Preview on Related Iron Oxide,” Front. Chem., vol. 7, no. June, pp. 112, 2019.